

## ANALYTICAL METHOD FOR COUPLING CALCULATIONS OF ROTATED IRIS COUPLED RESONATOR CAVITY

R. Kumar<sup>1, \*</sup>, P. Singh<sup>1</sup>, M. S. Bhatia<sup>2</sup>, and G. Kumar<sup>3</sup>

<sup>1</sup>Ion Accelerator Development Division, Bhabha Atomic Research Centre, Mumbai-400085, India

<sup>2</sup>Laser and Plasma Technology Division, Bhabha Atomic Research Centre, Mumbai-400085, India

<sup>3</sup>Department of Electrical Engineering, IIT Bombay, Mumbai-400076, India

**Abstract**—Iris type waveguide to cavity couplers are used to couple power to particle accelerator cavities. Waveguide to cavity coupling for arbitrarily oriented rectangular iris is analyzed using Bethe's small hole coupling theory. Magnetic moment of rotated iris is obtained by defining its dyadic magnetic polarizability. Power radiated by magnetic moment into the incoming waveguide is used for coupling calculations at arbitrary angle. A close agreement is found between the proposed theory, simulations and microwave measurements.

### 1. INTRODUCTION

Theory of coupling and radiation by small apertures in an infinite conducting wall has been studied by H. Bethe [1]. Further, for apertures of arbitrary shapes, Cohn has obtained electric and magnetic polarizability values by measurements in a chemical cell [2]. Bethe's theory has been used to obtain analytical expressions for waveguide to cavity coupling by Gao [3]. Gao has further extended the analysis from end coupled waveguide [3] to side coupled waveguide-cavity system [4]. For practical apertures of finite thickness, Gao has included attenuation coefficient to evaluate coupling coefficient of a waveguide-cavity coupled system.

Recently, first author has reported a novel way of changing the coupling coefficient by iris rotation in RF couplers for accelerator

---

*Received 19 July 2012, Accepted 19 September 2012, Scheduled 26 September 2012*

\* Corresponding author: Rajesh Kumar (rkthakur.iitk@yahoo.com).

cavities [5]. Concept of iris rotation is demonstrated in [5] using full wave simulations on commercial EM solver CST Microwave Studio (CST-MWS). In [5], a pill box cavity resonating at 350 MHz is studied for rotated rectangular and square iris coupling using simulations only. The work reported in present paper is distinct from [5] in mainly three ways. First, analytical expressions for rotated irises are derived from first principles using Bethe's theory. Second, other iris shapes like circular and elliptical are also analyzed apart from rectangular and square irises. Third, prototyping and microwave measurements are also carried out to verify the proposed analytical results. Considering the ease of fabrication, smaller coupler-cavity system at S band is analyzed here as compared to 350 MHz system in [5]. Iris rotation based technique is expected to be useful alternative to existing techniques based upon post fabrication machining for coupling adjustments in particle accelerator cavities [6]. Hence, a detailed analytical study of such coupling structures will be important.

In the context of accelerator cavities, Pascal has proposed an useful technique for calculating external  $Q$  numerically with lesser solver runs [7]. An equivalent circuit based approach for external  $Q$  calculations is reported in [8] but it doesn't consider rotated iris.

Though, iris at an angle has been used in waveguide directional couplers as a means to get different power divisions [9–11], the techniques used to obtain coupling values are either purely numerical or studied in the context of waveguide to waveguide coupling. There are many numerical studies on rotated iris coupling in the context of filters, e.g., [12] and EMC applications [13]. Bethe's theory has also been used recently to evaluate coupling in rectangular coaxial lines [14].

Bethe's original theory is modified by Collins by including reaction terms [15]. The modified theory is useful for waveguide-waveguide and waveguide-cavity coupling calculations in-order to obtain physically realizable equivalent circuits. The Collin's approach has been used for analytical studies on open resonator coupling [16] and cavity to cavity coupling [17]. However, in particle accelerator resonator cavities, information of external quality factor and coupling coefficient is good enough for describing their behavior at resonance because of single frequency operation. Hence, description of reaction terms for obtaining the physically realizable equivalent circuit may not be needed. As described in [3, 4], by using Bethe's original theory, coupling coefficient for iris coupled waveguide to cavity system can be obtained with reasonable accuracy.

We also use Bethe's original theory in this paper and arrive at analytical expressions for external  $Q$  and coupling of an iris at arbitrary orientation. We have chosen rectangular iris because of

its simplicity and regular use in practical waveguide-cavity coupled systems in accelerators. This is because of the fact that rectangular iris is easier to machine as compared to elliptical one. As shown in Section 3.1, rectangular iris also provides more coupling than circular and square iris. It also provides wider range of coupling variation with iris rotation as compared to square and circular iris shapes as discussed in Section 3.1.

Though, analytical expressions are not available for rectangular iris as opposed to elliptical iris, polynomial based methods are available [18–20]. We calculate the magnetic polarizability (i.e., longitudinal and transverse magnetic polarizability) of rectangular iris from these polynomial methods. These values are used to define dyadic magnetic polarizability of rectangular iris for arbitrary iris orientation in the plane of incoming waveguide. Attenuation based term is included to account for finite iris length [3, 21].

We evaluate external quality factor explicitly because it is the characteristic of coupler-cavity geometry and size only. It is independent of cavity material and its surface qualities. The external  $Q$  values for arbitrary iris angle are used to obtain coupling coefficient of the given system for a known intrinsic quality factor.

## 2. THEORY OF EXTERNAL $Q$ AND COUPLING CALCULATIONS

We consider a WR340 waveguide and rotatable rectangular iris for coupling power to a cylindrical pill box cavity. End coupled waveguide to cavity coupling is used in this study. The schematic of waveguide-cavity system along with rotatable iris cylinder is shown in Figure 1.

The incoming waveguide and cylindrical cavity operate in  $TE_{10}$  and  $TM_{010}$  mode respectively. The dimensions of waveguide, cavity and iris are also shown in Figure 1. The rectangular iris is cut inside a solid metallic cylinder. For the chosen dimensions, cavity's resonant frequency from analytical calculations comes out to be 2.373 GHz.

Iris length (major axis) is denoted by ' $l$ ' and width (minor axis) as ' $w$ '. Incoming waveguide length is ' $a$ ' and width is ' $b$ '. Cavity length is denoted by ' $L$ ' and diameter as ' $D$ '.

### 2.1. Magnetic Polarizability of Oriented Rectangular Iris

Iris oriented at angle ' $\theta$ ' in the plane of incoming waveguide is shown in Figure 2. The incoming waveguide cross-section is shown in  $x$ - $y$  co-ordinates whereas rotated iris is shown in  $u$ - $v$  co-ordinate system. It can be observed that  $u$ - $v$  co-ordinate system can be obtained by simple

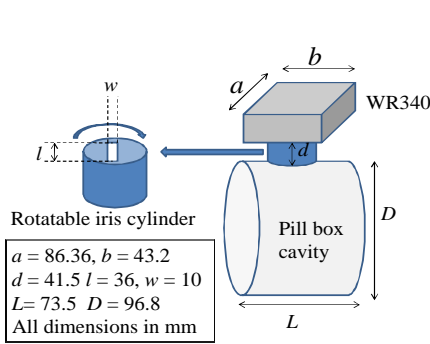


**Figure 1.** Schematic of iris coupled waveguide-cavity system.

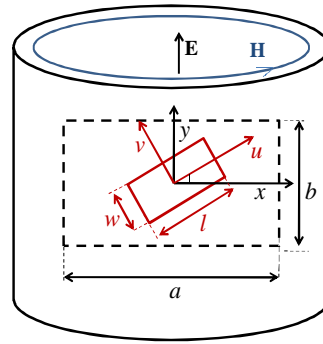


**Figure 2.** Cross-section of incoming waveguide and rotated iris (in  $x-y$  and  $u-v$  coordinate system respectively) coupling power to  $TM_{010}$  mode of cavity.

transformation of  $x-y$  system. Iris depth is not shown in Figure 2. Iris is shown in  $u-v$  coordinate system which is rotated by an angle ' $\theta$ ' w.r.t the  $x-y$  plane of incoming waveguide. Electric and magnetic fields of pill-box cavity's  $TM_{010}$  mode are shown as  $\mathbf{E}$  and  $\mathbf{H}$  respectively.

As there is no electric field perpendicular to iris plane, we will consider magnetic polarizability only. Magnetic polarizability ' $P_{m1}$ ' of rectangular iris at zero angle (also called longitudinal polarizability) is given by a polynomial expression as [19]:

$$P_{m1} = f_1 l^3 \quad (1a)$$

$$f_1 = \frac{0.132}{\ln\left(1 + \frac{0.660}{(w/l)}\right)} \quad (1b)$$

Here, ' $l$ ' is iris length and ' $w$ ' is iris width. Magnetic field orientation for longitudinal polarizability is shown in Figure 3(a). The iris orientation for transverse polarizability is shown in Figure 3(b).

Similarly, transverse magnetic polarizability of rectangular iris is given as [20]:

$$P_{m2} = f_2 l^3 \quad (2a)$$

$$f_2 = \frac{\pi}{16} \left(\frac{w}{l}\right)^2 \left(1.0 + 0.3221 \frac{w}{l}\right) \quad (2b)$$

Magnetic polarizability at an arbitrary angle can be defined by dyadic representation as [15]:

$$\bar{\mathbf{P}}_m = P_{m1} \mathbf{a}_u \mathbf{a}_u + P_{m2} \mathbf{a}_v \mathbf{a}_v \quad (3)$$

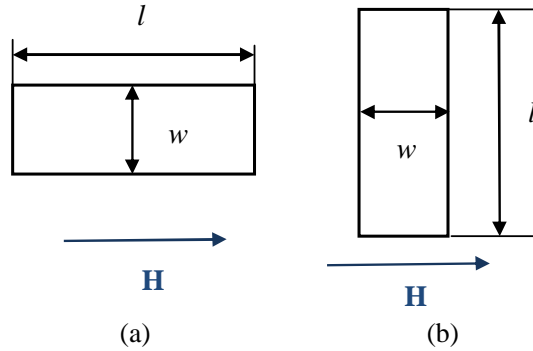


**Figure 3.** (a) Magnetic field and iris orientation for longitudinal polarizability. (b) Magnetic field and iris orientation for transverse polarizability.

The vectors  $\mathbf{a}_u$  and  $\mathbf{a}_v$  are unit vectors in  $u$ - $v$  plane. The  $\mathbf{a}_u$  is unit vector for  $u$  axis and  $\mathbf{a}_v$  is unit vector for  $v$  axis.

We will use this dyadic magnetic polarizability for external  $Q$  and coupling calculations using Bethe’s original theory.

### 2.2. Analytical Expressions for External $Q$ and Coupling Calculations

The normalized fields for  $TE_{10}$  mode of rectangular waveguide are given as [15]

$$\mathbf{E}_{10}^+ = \mathbf{e}_{10}e^{-j\beta z} \tag{4a}$$

$$\mathbf{H}_{10}^+ = (\mathbf{h}_{10} + \mathbf{h}_{z10}) e^{-j\beta z} \tag{4b}$$

$$\mathbf{E}_{10}^- = \mathbf{e}_{10}e^{j\beta z} \tag{4c}$$

$$\mathbf{H}_{10}^- = (-\mathbf{h}_{10} + \mathbf{h}_{z10}) e^{j\beta z} \tag{4d}$$

Here,

$$\mathbf{e}_{10} = -jk_oZ_oN \sin(\pi x/a) \mathbf{a}_y \tag{5a}$$

$$\mathbf{h}_{10} = -j\Gamma_{10}N \sin(\pi x/a) \mathbf{a}_x \tag{5b}$$

$$\mathbf{h}_{z10} = \frac{N\pi}{a} \cos(\pi x/a) \mathbf{a}_z \tag{5c}$$

$$\mathbf{N} = (-2/(abk_oZ_o\Gamma_{10}))^{1/2} \tag{5d}$$

Here,  $Z_o$  is the intrinsic impedance of free space,  $k_o$  the free space propagation constant, and  $\Gamma_{10}$  the waveguide propagation constant.

For all field equations discussed here, time dependence is not explicitly shown.

Let us assume that cavity's magnetic field at aperture location is  $\mathbf{H}$ . It is also assumed that cavity field is aligned with  $x$ -axis on the aperture surface. Magnetic moment ( $\mathbf{M}$ ) produced by dyadic magnetic polarizability can be written as [15]:

$$\mathbf{M} = \bar{\mathbf{P}}_m \cdot \mathbf{H} \quad (6a)$$

After replacing polarizability value from Equation (3) into Equation (6a), we get

$$\mathbf{M} = (P_{m1}\mathbf{a}_u\mathbf{a}_u + P_{m2}\mathbf{a}_v\mathbf{a}_v) H\mathbf{a}_x \quad (6b)$$

After simplification, (6b) becomes

$$\mathbf{M} = (P_{m1} \cos(\theta)\mathbf{a}_u + P_{m2} \sin(\theta)\mathbf{a}_v) H \quad (6c)$$

This means that cavity field is effectively splitting to two orthogonal polarizations in the rotated iris. In  $u$ - $v$  coordinate system, ' $u$ ' polarization couples to cavity field magnitude of  $H \cos(\theta)$  whereas ' $v$ ' polarization to field magnitude of  $H \sin(\theta)$ .

This magnetic dipole will radiate into the incoming waveguide. The induced magnetic field ( $H_o$ ) in the incoming waveguide's cross-section can be written as [15, 16]

$$H_o = (j\omega\mu_o\mathbf{H}_{10}^+ \cdot \mathbf{M}) H_{10}^- \cdot \mathbf{a}_x \quad (7a)$$

The above expression reduces to:

$$H_o = (j\omega\mu_o\mathbf{h}_{10}^2) \mathbf{M} \cdot \mathbf{a}_x \quad (7b)$$

After substituting Equation (5b) into above equation, it reduces to

$$H_o = \frac{-2j\Gamma_{10}\mathbf{M} \cdot \mathbf{a}_x}{ab} \quad (7c)$$

After replacing magnetic moment's value from Equation (6c) into Equation (7c), we obtain

$$H_o = \frac{-2j\Gamma_{10} (P_{m1} \cos(\theta)\mathbf{a}_u \cdot \mathbf{a}_x + P_{m2} \sin(\theta)\mathbf{a}_v \cdot \mathbf{a}_x) H}{ab} \quad (8)$$

The  $H_o$  is  $\mathbf{x}$  component of waveguide's maximum magnetic field.

After simplification, Equation (8) reduces to

$$H_x = \frac{-2j\Gamma_{10} (P_{m1} \cos^2(\theta) + P_{m2} \sin^2(\theta)) H}{ab} \quad (9)$$

Corresponding maximum electric field  $E_y$  at the center of waveguide can be obtained from waveguide impedance ( $Z_{TE}$ ) given below [22]

$$Z_{TE} = \frac{E_y}{H_x} = \frac{k_o Z_o}{\Gamma_{10}} \quad (10)$$

With the information obtained so far, the average power radiated into the waveguide can be calculated as [22]

$$P_{rad} = \frac{E_y H_x ab}{4} \tag{11a}$$

Power radiated into the waveguide can also be written as

$$P_{rad} = \frac{H_x^2 ab Z_{TE}}{4} \tag{11b}$$

From Equations (9), (10) and (11b), we get

$$P_{rad} = \frac{\Gamma_{10} k_o Z_o (P_{m1} \cos^2(\theta) + P_{m2} \sin^2(\theta))^2 H^2}{ab} \tag{11c}$$

External quality factor ( $Q_{ext}$ ) can be written as

$$Q_{ext} = \frac{\omega_o U}{P_{rad}} \tag{12a}$$

Here,  $\omega_o$  is resonant frequency and  $U$  is energy stored in cavity.

After placing Equation (11c) into Equation (12a), we obtain

$$Q_{ext} = \frac{\omega_o U ab}{\Gamma_{10} k_o Z_o H^2 (P_{m1} \cos(\theta)^2 + P_{m2} \sin(\theta)^2)^2} \tag{12b}$$

This expression is obtained for zero iris thickness. For iris of thickness  $d$ , an attenuation term is included for the magnetic field [3, 21]. If  $\alpha$  is attenuation coefficient of dominant  $TE_{10}$  mode of rectangular iris, Equation (12b) can be written for iris of finite thickness as

$$Q_{ext} = \frac{\omega_o U ab}{\Gamma_{10} k_o Z_o H^2 \exp(-2\alpha d) (P_{m1} \cos(\theta)^2 + P_{m2} \sin(\theta)^2)^2} \tag{12c}$$

Intrinsic quality factor ( $Q_o$ ) of the resonator can be written as [22]

$$Q_o = \frac{\omega_o U}{P_o} \tag{13}$$

Here,  $P_o$  is energy dissipated on the cavity walls. Coupling coefficient ' $\beta$ ' can be calculated as [22]

$$\beta = \frac{Q_o}{Q_{ext}} \tag{14a}$$

After using Equations (12c), (13) and (14a), we get

$$\beta = \frac{\Gamma_{10} k_o Z_o \exp(-2\alpha d) (P_{m1} \cos^2(\theta) + P_{m2} \sin^2(\theta))^2 H^2}{ab P_o} \tag{14b}$$

After simplification, (14b) can be written as

$$\beta = \left( \sqrt{\beta_1} \cos^2(\theta) + \sqrt{\beta_2} \sin^2(\theta) \right)^2 \quad (14c)$$

Here,

$$\beta_1 = \frac{2\Gamma_{10}k_oZ_o \exp(-2\alpha d) (P_{m1})^2 H^2}{abP_o} \quad (14d)$$

$$\beta_2 = \frac{2\Gamma_{10}k_oZ_o \exp(-2\alpha d) (P_{m2})^2 H^2}{abP_o} \quad (14e)$$

From Equation (14c), we can observe that the coupling contributions from longitudinal and transverse polarizabilities get combined to produce the overall coupling. The contribution from longitudinal coupling is given in Equation (14d) whereas the contribution from transverse coupling is shown in Equation (14e).

### 2.3. Special Cases

#### 2.3.1. Elliptical Iris

Magnetic polarizability of elliptical iris with magnetic field parallel to longer dimension (i.e., longitudinal polarizability) is given as [15]

$$P_{m1} = \frac{\pi l_1^3 e_o^2}{3(K(e_o) - E(e_o))} \quad (15)$$

Here,  $l_1$  is semi-major axis of ellipse and  $l_2$  is semi-minor axis.  $K(e_o)$  and  $E(e_o)$  are elliptic integrals of first and second order respectively. Also, eccentricity ' $e_o$ ' is given as

$$e_o = \sqrt{1 - \frac{l_2^2}{l_1^2}} \quad (16)$$

As a special case, for zero degree iris orientation, Equation (12c) reduces to

$$Q_{ext1} = \frac{\omega_o U ab}{\Gamma_{10}k_oZ_o \exp(-2\alpha d) H^2 P_{m1}^2} \quad (17)$$

From (14a), (15) and (17), we get

$$\beta_1 = \frac{\Gamma_{10}k_oZ_o\pi^2 \exp^{-2\alpha d} l_1^6 e_o^4 H^2}{9ab(K(e_o) - E(e_o))^2 P_o} \quad (18)$$

This equation is the same as that reported in [4]. Transverse coupling value can be obtained by same procedure. This is a validation of proposed expressions.

### 2.3.2. Circular Iris

Coupling for circular iris with radius ‘ $r$ ’ can be obtained by similar procedure. The magnetic polarizability of circular iris is given as

$$P_{m1} = \frac{4r^3}{3} \quad (19)$$

As circle is azimuthally symmetrical, it is interesting to note that coupling for zero and 90 degrees is same. Due to this fact, Equation (14c) can be written as

$$\beta = \left( \sqrt{\beta_1} (\cos^2(\theta) + \sin^2(\theta)) \right)^2 \quad (20a)$$

After simplification, Equation (23) reduces to:

$$\beta = \left( \sqrt{\beta_1} \right)^2 = \beta_1 \quad (20b)$$

This implies that coupling for circular iris remains constant with iris rotation in the plane of incoming wave-guide cross-section. This result is quite logical and thus validates the proposed theoretical procedure.

### 2.3.3. Square Iris

For a square iris also, the coupling for zero and 90 degrees iris orientation will be the same. This happens because the longitudinal and transverse polarizability values are same owing to equal arm lengths [19,20]. Hence, we will get the same result as that of Equation (20b). This implies that coupling for square iris should remain constant with iris rotation.

However, as reported in [5], there is about  $+ - 10\%$  variation in the beginning and end of rotation range for square iris. This is attributed to the fact that square iris simulated in [5] is conformal to the cavity surface. Because of curved nature of cavity surface, effective iris thickness changes during its rotation range. Other factor causing the small variation in coupling of square iris can be field non-uniformity at waveguide end. For large apertures, the non-uniform nature of waveguide’s  $TE_{10}$  fields leads to errors as proposed theory assumes uniform field.

### 2.3.4. Rectangular Iris with Low Aspect Ratio ( $w/L \ll 1$ )

For rectangular iris with small aspect ratio, it is noticed that transverse coupling is several orders of magnitude lower than longitudinal coupling ( $\beta_2 \ll \beta_1$ ). This happens because of lower polarizability ( $P_{m2} \ll P_{m1}$ ) and higher attenuation in transverse slot. Hence, after

neglecting the contribution of transverse term, Equation (12c) and Equation (14c) can be written as:

$$Q_{ext} = \frac{\omega_o U ab}{\Gamma_{10} k_o Z_o \exp^{(-2\alpha d)} H^2 P_{m1}^2 \cos^4(\theta)} \quad (21)$$

$$\beta(\theta) = \left( \sqrt{\beta_1} \cos^2(\theta) \right)^2 = \beta_1 \cos^4(\theta) \quad (22)$$

#### 2.4. Calculation of External $Q$ and Coupling Coefficient

As the resonant frequency of the structure is known analytically, we need the value of maximum magnetic field  $H$  on cavity surface. The maximum magnetic field on cavity surface for 1 J of energy stored can also be obtained analytically for a pill box cavity. All other parameters required for  $Q_{ext}$  calculations from Equation (12c) are known analytically.

As practical structures are complex, one may need at least one EM modal solver run to get the value of  $H$  for 1 J of energy stored. For example, in our case, this value is obtained from one CST Modal solver run and is found to be 65000 A/m. From this  $H$  value, we could obtain  $Q_{ext}$  for any iris orientation from Equation (12c).

Further, if intrinsic quality factor is known, coupling coefficient can be obtained by simply dividing it with  $Q_{ext}$ . By using  $H$ ,  $\omega_o$  and  $P_o$  values from one modal solver run, we could calculate  $Q_{ext}$  and  $\beta$  for any arbitrary iris orientation.

We used the  $Q_{ext}$  values obtained from Equation (12c) and  $\beta$  values from (14) and compared them with measurements and simulated values. The comparison is discussed in next section.

### 3. FULL WAVE SIMULATIONS AND EXPERIMENTAL RESULTS

#### 3.1. Full Wave Simulations

Considering the ease of fabrication, it is decided to demonstrate the concept experimentally on a small cavity operating in S band.

A cylindrical cavity is modeled using commercial EM solver CST-MWS. The analytical value of resonant frequency for the cavity dimensions given in Figure 1 comes out to be 2.373 GHz. The simulated value of resonant frequency for  $TM_{010}$  mode is 2.360 GHz. Slight decrease in simulation values ( from analytically calculated value of 2.373 GHz) is because the RF port, iris and incoming waveguide are also included in the simulation.

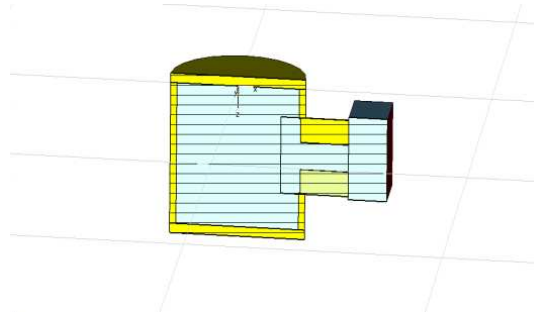


Figure 4. Cut-view of simulation model.

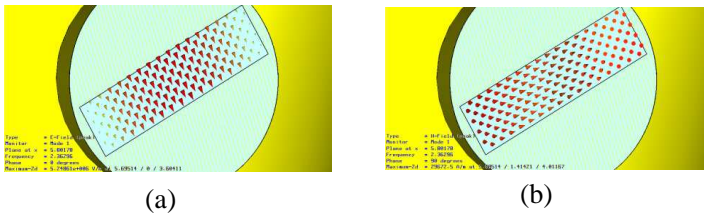


Figure 5. (a) Simulated arrow plots of  $E$  field in the rotated iris. (b) Magnetic field arrow plots in the rotated iris.

The coupler-cavity simulation model is shown in Figure 4. For each Eigen Mode solver run of CST MWS, iris is rotated in the plane of incoming WR340 waveguide. Conducting boundary with  $\sigma = 5.8e7S/m$  is used. Intrinsic quality factor of approx. 22,000 is obtained during simulations for the entire rotation range. External  $Q$  value is obtained from the CST-MWS Modal Solver for every 15 degrees iris rotation by defining a matched boundary at waveguide port.

In order to have a better view of fields in the rotated iris, arrow plots of simulated  $\mathbf{E}$  and  $\mathbf{H}$  fields are shown in Figure 5(a) and Figure 5(b), respectively.

Full wave simulations are performed for rectangular, elliptical, square and circular iris shapes. As shown in Figure 1, rectangular iris of length 36 mm and with 10 mm is chosen. To keep the sizes comparable, elliptical iris with major axis of 36 mm and minor axis of length 10 mm is considered. Similarly, diagonal of square iris and diameter of circular iris are chosen to be 36 mm.

The plots for variation of external  $Q$  with iris rotation are given in Figure 6(a). It should be noted that external  $Q$  is plotted on log scale because of several orders of variation over the rotation range.

Also, coupling coefficient variation with rotation angle is shown in Figure 6(b). It is important to observe that rectangular iris is plotted on the left scale whereas other iris shapes are plotted on the right scale because of orders of magnitude difference in coupling values.

We can observe from these plots that square and circular irises give very low coupling as compared to rectangular and elliptical irises. Moreover, square and circular irises are not useful for rotatable iris based coupling variation schemes as there is practically no coupling variation over the entire rotation range. The rectangular iris gives more coupling than elliptical iris for chosen dimensions. Hence, we chose rectangular iris for validation with measurements as it provides more coupling, wide range and is easier to fabricate.

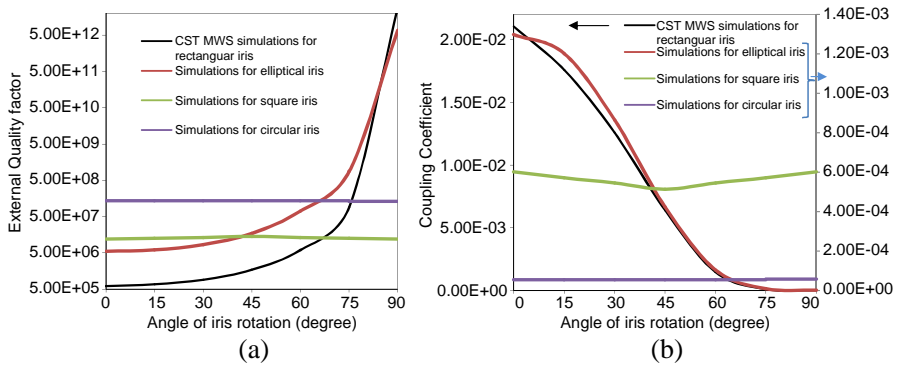


**Figure 6.** (a) External  $Q$  simulation results for different iris shapes. (b) Coupling coefficient simulation results for different iris shapes.



**Figure 7.** (a) Iris cylinder with rectangular iris. (b) Cavity connected to VNA through WR340-N Type adapter and auxiliary port for transmission measurements.

### 3.2. Measurements for External $Q$ and Coupling Coefficient

The coupler parts and fabricated cavity are shown in Figure 7(a) and Figure 7(b) respectively. The incoming waveguide port from WR340 to N Type adapter is blocked with a stainless steel (SS) flange. The SS flange has a provision for mounting the iris at the center. The iris part can be rotated with respect to the waveguide cross-section. The SS flange is also provided with holes so that it can be mounted on to the cavity port. Cavity port diameter is 40 mm. The Cavity, ports and iris are made with SS and plated with Cu.

In order to measure the coupling with transmission method [23], a small port of 10 mm diameter is provided on the cavity. A small loop made of an N Type connector is mounted on this auxiliary port. In order to feed the microwave power to WR340 waveguide, a WR 340 to N Type adapter is used. Measurements are performed with Vector Network Analyzer (VNA) of R&S ZVB4 series.

The coupling coefficient of auxiliary loop coupled cavity can be written as [22]:

$$\beta_a = \frac{R}{Z_o} \quad (23)$$

Here,  $R$  is the impedance of cavity at resonance, and  $Z_o$  is 50 Ohms. Also, the reflection coefficient of coupled cavity at resonance is given as:

$$S_{11} = \frac{\frac{R}{Z_o} - 1}{\frac{R}{Z_o} + 1} \quad (24)$$

A reflection measurement ( $S_{11}$ ) at auxiliary port is used to calculate the coupling coefficient from Equations (23) and (24).

Hence, coupling of auxiliary loop ( $\beta_a$ ) is found to be 0.7 from measured  $S_{11}$  of 15 dB. The relevant equations for  $Q_o$  and  $Q_{ext}$  calculations from measurements are given as [23]:

$$Q_o = Q_L (1 + \beta_a + \beta_{ext}) \quad (25)$$

$$Q_{ext} = \frac{4\beta_a Q_L}{1 + \beta_a} 10^{|S_{21} \text{ dB}|/10} \quad (26)$$

Loaded quality factor  $Q_L$  is obtained from transmission measurements using 3 dB method.  $Q_o$  of fabricated cavity is calculated from Equation (25) and it came out to be 7219. As found from reflection measurements, coupling coefficient of iris coupled waveguide to cavity system ( $\beta_{ext}$ ) is very low and hence neglected for calculating  $Q_o$  from Equation (25). For each measurement, iris coupler is rotated and corresponding transmission magnitude is noted. Finally, unknown

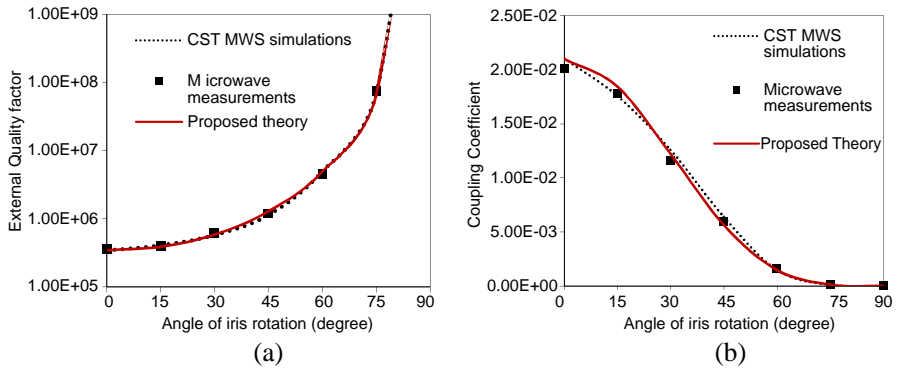


**Figure 8.** (a) External  $Q$  variation of simulated, measured, and proposed analytical results for different rotation angle of rectangular iris. (b) Coupling variation of simulated, measured, and proposed analytical results for different rotation angle of rectangular iris.

$Q_{ext}$  and coupling coefficient are calculated from Equation (26) and Equation (14a) respectively.

The external  $Q$  and coupling coefficient values are obtained from measurements and compared with simulations and theoretically calculated values. For coupling coefficient calculations, measured value of  $Q_o$  is used for comparative analysis.

The plots for external  $Q$  and coupling coefficient variation with iris rotation are shown in Figure 8(a) and Figure 8(b) respectively. A close agreement is found between simulations, measurements and proposed theory. Maximum mismatch between theoretical and measured values as compared to simulations is found to be less than 10%.

Hence, proposed theory shows good agreement with simulations and measurements in terms of trend and absolute values.

It will be important to discuss the possible sources of measurement errors and uncertainties. The external  $Q$  measurements are very sensitive to  $S_{21}$  magnitude especially at higher angles (because of very weak coupling). This error is found to be around 3–4% at higher angles with  $\pm 0.1$  dB change in  $S_{21}$  magnitude. The angle of iris rotation was adjusted within accuracy of  $\pm 1$  degree during measurements. The dimensional accuracy of fabricated components was within  $\pm 100$  microns. The coupling is highly sensitive to iris length and can result in around 1.5–2% change of coupling for said tolerances. The cavity surface is not exactly planar at iris interface as assumed in proposed theory. All of these factors may be responsible for difference in theoretical, simulated and measured results.

#### 4. CONCLUSIONS

Analytical expressions are derived for waveguide to cavity coupling with rotated rectangular iris. From proposed generalized expressions for arbitrary iris orientation, analytically known results for non-rotated elliptical iris could be obtained as a special case. Other iris shapes like square and circular are also analyzed with proposed theory and simulations. The results are validated with full wave simulations and measurements. These expressions will be useful in reducing the design time of RF couplers for accelerator cavities and other novel devices based upon rotated iris coupling. Proposed theoretical results will also be useful in establishing the coupling scaling laws for an iris at arbitrary angle.

#### ACKNOWLEDGMENT

The authors are thankful to Dr. S. Kailas for his keen interest and encouragement for development of novel coupling schemes at Ion Accelerator Development Division (IADD), BARC. First author would also like to thank Dr. J. Gao, IHEP, China for useful discussions on waveguide to cavity coupling. We also acknowledge the useful discussions with Dr. S. R. Jain, NPD, BARC.

#### REFERENCES

1. Bethe, A., "Theory of diffraction by small holes," *Physical Review*, Vol. 66, 163–182, Oct. 1944.
2. Cohn, S. B., "Determination of aperture parameters by electrolytic-tank measurements," *Proceedings of the IRE*, Vol. 66, 1416–1421, Nov. 1951.
3. Gao, J., "Analytical formula for the coupling coefficient  $\beta$  of a cavity-waveguide coupled system," *Nuclear Instruments and Methods*, Vol. A309, 5–10, 1991.
4. Gao, J., "Analytical determination of the coupling coefficient of waveguide cavity coupling systems," *Nuclear Instruments and Methods*, Vol. A481, 36–42, 2002.
5. Kumar, R., "A novel method for variable coupling using iris rotation in RF couplers," *Nuclear Instruments and Methods*, Vol. A600, 534–537, 2009.
6. Balleyguier, P. and M. Painchault,, "Design of RF power input ports for IPHI RFQ," *Proc. European Particle Accelerator Conf. EPAC*, 2124, Paris, 2002.

7. Balleyguier, P., "External  $Q$  studies for APT cavity couplers," *Proc. Linear Accelerator Conf. LINAC*, 133–135, Chicago, 1998.
8. Kamigaito, O., "Circuit model representation of external- $Q$  calculation," *Phys. Rev. ST Accl. Beams*, Vol. 9, 062003, 2006.
9. Rengarajan, S. R., "Analysis of a centered-inclined waveguide slot coupler," *IEEE Trans. Microwave Theory Tech.*, Vol. 37, No. 5, 884–889, May 1989.
10. Rengarajan, S. R., "Characteristics of a longitudinal/transverse coupling slot in crossed rectangular waveguides," *IEEE Trans. Microwave Theory Tech.*, Vol. 37, No. 8, 1171–1177, Aug. 1989.
11. Nesterenko, M. V., V. A. Katrich, Y. M. Penkin, and S. L. Berdnik, "Analytical methods in theory of slot-hole coupling of electrodynamic volumes," *Progress In Electromagnetics Research*, Vol. 70, 79–174, 2007.
12. Accatino, L., G. Bertin, and M. Mongiardo, "A four pole dual mode elliptic filter realized in circular cavity," *IEEE Trans. Microwave Theory Tech.*, Vol. 44, No. 12, 2680–2687, Dec. 1996.
13. Khan, Z. A., C. F. Bunting, and M. D. Deshpande, "Shielding effectiveness of metallic enclosures at oblique and arbitrary polarizations," *IEEE Trans. Electromagnetic Compatibility*, Vol. 47, No. 1, 112–122, Feb. 2005.
14. Saito, Y. and D. S. Filipovic, "Analysis and design of monolithic rectangular coaxial lines for minimum coupling," *IEEE Trans. Microwave Theory Tech.*, Vol. 55, No. 12, 2521–2530, Dec. 2007.
15. Collins, R. E., *Field Theory of Guided Waves*, IEEE Press, 1996.
16. Mongia, R. K. and R. K. Arora, "Equivalent circuit parameters of an aperture coupled open resonator cavity," *IEEE Trans. Microwave Theory Tech.*, Vol. 41, No. 8, 1245–1250, Aug. 1993.
17. Roy, R. and O. Shanker, "Calculation of inter cavity coupling coefficient for side coupled standing wave linear accelerator," *IEEE Trans. Microwave Theory Tech.*, Vol. 41, No. 6, 1233–1235, Jan. 1993.
18. McDonald, N. A., "Polynomial approximations for the electric polarizabilities of some small apertures," *IEEE Trans. Microwave Theory Tech.*, Vol. 33, No. 11, 1146–1149, Nov. 1985.
19. McDonald, N. A., "Simple approximations for the longitudinal magnetic polarizabilities of some small apertures," *IEEE Trans. Microwave Theory Tech.*, Vol. 36, No. 7, 1141–1144, Jul. 1988.
20. McDonald, N. A., "Polynomial approximations for the transverse magnetic polarizabilities of some small apertures," *IEEE Trans. Microwave Theory Tech.*, Vol. 35, No. 1, 20–23, Jan. 1987.

21. McDonald, N. A., "Electric and magnetic coupling through small apertures in shield walls of any thickness," *IEEE Trans. Microwave Theory Tech.*, Vol. 20, 689–685, Oct. 1972.
22. Pozar, M., *Microwave Engineering*, 2nd Edition, 333, Wiley, New York, 2003.
23. Kang, Y., S. Kim, M. Doleans, I. E. Campisi, M. Stirbet, P. Kneisel, G. Ciovati, G. Wu, and P. Yla-Oijala, "Electromagnetic simulations and properties of the fundamental power couplers for the SNS superconducting cavities," *Proc. Particle Accelerator Conference, (PAC-2001)*, 1122–1124, Jun. 2001.